

Hybrid manufacturing scheme for metal using robot and CNC machine

Meng Li, He Lyu, Xiangbao Song, Zexiang Li, *Life Fellow, IEEE*

Abstract—This paper presents a hybrid layered manufacturing process combining the best features of both robotic additive manufacturing and CNC machining approaches. Compare to the conventional manufacturing process, the advantage of the hybrid manufacturing system is that material can be added and subtracted, ad infinitum until a desirable product has been achieved. A slicing algorithm is developed to generate the contour tool-paths along the boundary of the designed model, and these contour curves of each sliced layer are offset to preserve geometrical accuracy. For the internal area of the layer, zigzag tool-paths are adopted to simplify computing processes and speed up fabrication. The hardware integration of this system is described in detail, including the design and use of each subsystem, and the control scheme of the entire system. Finally, a series of experiments are carried out to obtain suitable processing parameters, and an industrial case is conducted subsequently proving the viability of the hybrid system.

Index Terms—hybrid manufacturing, additive manufacturing, industrial robot

I. INTRODUCTION

Additive manufacturing(AM) has been used in various sectors for single-unit production successfully, owing to the lots of advantages over conventional manufacturing that the process provides, such as

- Additive Manufacturing can build highly complex structures, while keeping stable and extremely light.
- It provides a high degree of design freedom, the optimisation and integration of functional features, the manufacture of small batch sizes at reasonable unit costs and a high degree of product customisation even in serial production.
- It enables a design-driven manufacturing process - where design determines output and not the other way around.

AM offers a total automation solution in converting the virtual models into physical ones. AM could also realise real 3D (6-axis controlled) motion when combined with industrial robots. There are many trial applications being done[1][2][3][4], which show the advantages of robotic additive manufacturing compared with articulated or other kinematic structures. Advantages of additive manufacturing with robots can be listed as below

- Fast process implementation
- Easy and error free robotic programming
- Optimal use of the robot's kinematics for superior motion control

Meng Li and H. Lyu are with the Department of Electrical and Computer Engineering, Hong Kong University of Science and Technology, Clear Water Bay, Kowloon, Hong Kong. e-mail: mliaz,hlv@ust.hk.

Xiangbao Song is with Googol Technology Limited, Shenzhen, China e-mail:song.xb@googletech.com.

Zexiang Li is with the Department of Electrical and Computer Engineering, Hong Kong University of Science and Technology Clear Water Bay, Kowloon, Hong Kong. e-mail: eezxli@ust.hk.

- Build larger components that are possible with conventional enclosed additive devices
- Easy to integrate additive manufacturing with other conventional automated production systems, such as machining.

However, AM is still restricted because of low accuracy and long production time, comparing with CNC machining[5]. On the other hand, CNC machining has the difficulties in machining complex structures due to tool accessibility.

Based on the problems mentioned above, hybrid manufacturing, the combination of at least two manufacturing processes, is becoming hot topical for researchers in manufacturing area. To enhance their advantages while minimise their disadvantages is the purpose of developing the hybrid processes. [1][6]. The combination of additive processes and CNC machining may provide a new substantial solution to both high accuracy and rapid prototyping.

In this paper, a hybrid manufacturing method is implemented by combining a robotic additive manufacturing station with a CNC machine. A slicing algorithm and a mixed tool-path generation algorithm are developed to generate contour tool paths along the boundary. Then a robust curve offset algorithm is proposed to offset each sliced layer to preserve geometrical accuracy. The internal area of each layer is fabricated by zigzag tool paths. Then the implementation of hardware station is introduced in detail which includes a laser system, robot, CNC machine and positioning system.

The rest of the paper is organized as follows: In section II, an overview of the hybrid system is given. In section III, mesh slicing algorithm is discussed. Then the path generation algorithm is presented in section IV. In section V, the implementation of hardware station is introduced in detail. The experiments were designed to demonstrate the algorithm in section VI, and finally, section VII concludes this paper.

II. AUTOMATED MANUFACTURING SYSTEM

A. Hybrid Manufacturing System

An automated process planning algorithm for a manufacturing system from CAD model inputs to finished parts is shown in Fig. 1. Several modules are essential including model segmentation, model slicing and path planning, laser parameter setting, post-process machining, robot code generation module, and the CNC Gcode generation module.

Firstly, the 3D CAD model in STL format is partitioned into several sub-models based on its geometric features by segmentation modules. Segmentation algorithm of 3D STL model has been widely reported[7]. In this paper, the algorithm based on shape diameter-function(SDF) value is used to partition a mesh model[8]. After the slicing direction and thickness are assigned

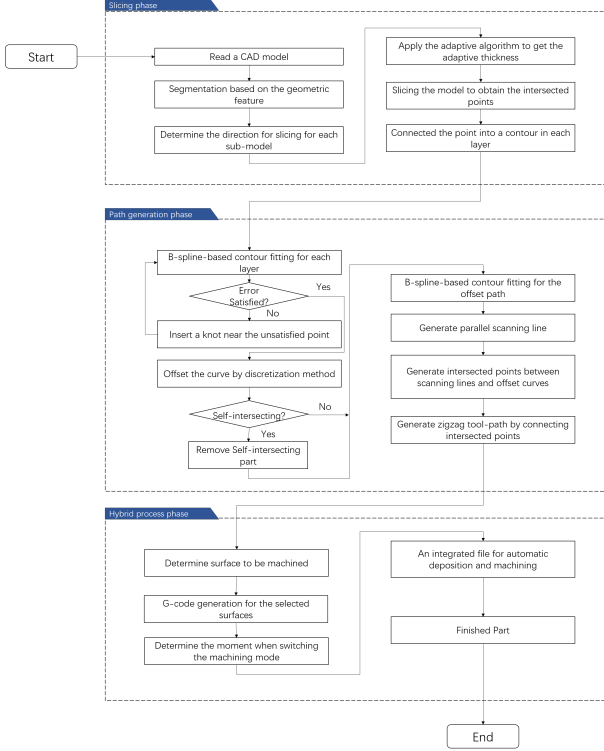


Fig. 1: Steps of Hybrid Manufacturing

for each sub-model, the slicing algorithm is performed to slice each sub-model layer by layer.

In the path planning, a B-spline approximate fitting algorithm is designed to fit the contour polygon and guarantee a satisfactory appropriate error. Then, a robust curve offset algorithm is applied to preserve model boundary accuracy. Subsequently, zigzag tool-paths are generated for the inner area of the model with the offset curves.

In the hybrid process phase, the corresponding Gcode is generated. Then based on the processing requirements, the moment of switching processing mode between the deposition mode and machining mode is determined. Finally, the station will perform the control file to add and subtract the materials automatically until the outcome has been achieved.

III. MESH SLICING

A. Mesh Slicing

The function of mesh slicing algorithm is to generate each layer's contour by intercepting the layers of model. As the triangles in the mesh data are in random order, the basic idea is to intercept the triangles with a plane of the mesh data. The problem of intersection can be solved easily, which results in a line segment as shown in Fig. 2a. However, the key problem is to find the intersecting triangles of each plane efficiently.

Chalasani and Grogan[9] test the cutting plane with every triangle. Obviously, this is a naive slicing algorithm for there are excessive, unnecessary intersection tests. Thus, to improve the efficiency, a mesh slicing algorithm and a triangle filter algorithm are designed by reducing the tests of triangle-plane intersection.

Algorithm 1: Mesh Slicing

Input: Mesh data: $T = (T_1, T_2, \dots, T_n)$,

Cutting Plane: z .

Output: Segments:

$$S = (S_1, S_2, \dots, S_k)$$

```

1: function MeshSlicing( $T, z$ )
2:    $F = \text{TriangleFliter}(T, z)$ 
3:    $\text{Segments.clear}()$ 
4:   for  $t \in F$  do
5:      $S = \text{Intersection}(t, z);$ 
6:      $\text{Segments.pushback}(S)$ 
7:   end for
8:   return Segments
9: end function
  
```

The inputs of the mesh slicing algorithm are the triangle mesh data and the cutting layer, and the output is a set of segments. First, a triangle filter is used to get a group of triangles that contain edges cross the current layer, which can improve the efficiency of the algorithm by avoiding unnecessary intersection tests. Then for each triangle in the group, a segment can be get by the plane-triangle intersection test. The triangle filter algorithm can find the triangles that intersect with cutting layer, so that the slicing algorithm is optimised compared with the unsorted triangle sets.

Algorithm 2: Triangle Filter

Input: Mesh data: $T = (T_1, T_2, \dots, T_n)$,

Cutting Plane: z .

Output: Lists of triangles of the target layer

$$G = (T_1, T_2, \dots, T_k)$$

```

1: function TriangleFilter( $T, z$ )
2:   //remove triangles lower than cutting layer
3:    $L_1 = \text{SortbyTzmax}(M)$ 
4:    $F_1 = \text{FliterbyTzmax}(L_1, z)$ 
5:   //remove triangles higher than cutting layer
6:    $L_2 = \text{SortbyTzmin}(F_1)$ 
7:    $F_2 = \text{FliterbyTzmin}(L_2, z)$ 
8:   return  $G = F_2$ 
9: end function
  
```

B. Curve Construction

In a mesh data, an edge intersects the cutting plane twice at same intersection point for it is shared by two triangles. For example, in Fig. 2b, the edge in the middle is shared by triangles T_1 and T_2 . Thus, the intersection segments $q_1^{T_1} q_2^{T_1}$ and $q_1^{T_2} q_2^{T_2}$ is connected by the same points $q_2^{T_1} (q_1^{T_2})$. The Proposed contour construction algorithm as shown in Algorithm 3 employ this feature and a k-d tree is used to connect the segments into a contour.

C. Slicing Algorithm

Finally, the slicing algorithm can be summarised as follow. By cutting the surface, a set of segments is obtained with

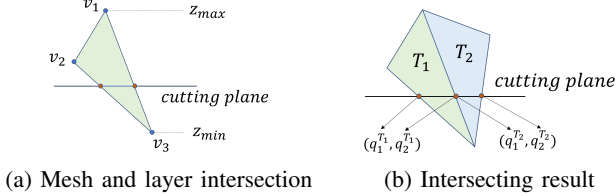


Fig. 2: Mesh Intersection

Algorithm 3: Contour Construction**Input:** Segments:

$$S = (S_1, S_2, \dots, S_k)$$

Output: Path:

$$Path = (C_1, C_2, \dots, C_n)$$

```

1: function ContourCstrct(S)
2:   tree = kdTreeBuild(S)
3:   while size(S) > 0 do
4:     C.clear()
5:     seg = S.pop()
6:     C.push(seg)
7:     while true do
8:       seg1 = kdTreeSearch(seg)
9:       if seg1.isSearched()||seg1 = null then
10:        break
11:       end if
12:       C.push(seg1)
13:     end while
14:     Path.push(C)
15:   end while
16:   return Path = (C_1, C_2, \dots, C_n)
17: end function
```

the mesh slicing method, and then join these segments into curves with curve construction algorithm. Repeat these two steps layer by layer until the whole model is sliced.

Algorithm 4:Slicing Algorithm**Input:** Mesh Model: M ,Offset: d ,**Output:** Layers

```

1: function Slicing(M, d, IsA)
2:   CCP = {}
3:   z = M.zmin
4:   while z < M.zmax do
5:     Segments = MeshSlicing(M, z)
6:     CCP.pushback(ContourCstrct(Segments))
7:     z += d
8:   end while
9:   return CCP
10: end function
```

IV. PATH PLANNING

Path planning generates reasonable deposit paths automatically for arbitrary contour obtained from the slicing module. For an automated AM system, one of the crucial requirements is the development of an elaborate path planning strategy.

A mixed tool-path algorithm combining zigzag and contour tool-paths was developed to ensure both requirements of build efficiency and geometrical accuracy. To improve the geometrical quality of a product model, the contour tool-paths are used to fabricate the area along the boundary of each sliced layer. To improve the efficiency, the zigzag tool-paths are used to fabricate the interior area of the model .

A B-spline curve is used to fit the intersected points of the sliced layer, and a fitting algorithm is developed.

A. B-spline Based Contour Curve Representation

B-spline, or basis spline, is widely used in the curves and surfaces representation. A B-spline curve is defined as a linear combination of control points P_i and B-spline basis functions $N_{i,p}(u)$ given by

$$C(u) = \sum_{i=0}^n P_i N_{i,p}(u) \quad (1)$$

The i th B-spline [11] basis function of p -degree denote by $N_{i,p}(u)$ is defined

$$N_{i,0}(u) = \begin{cases} 1 & \text{if } u_i \leq u \leq u_{i+1} \\ 0 & \text{otherwise} \end{cases} \quad (2)$$

$$N_{i,p}(u) = \frac{u - u_i}{u_{i+p} - u_i} N_{i,p-1}(u) + \frac{u_{i+p+1} - u}{u_{i+p+1} - u_{i+1}} N_{i+1,p-1}(u) \quad (3)$$

The basis function defined on a knot vector U , where u_i is called a knot.

$$U = \{u_0, \dots, u_i, \dots, u_n\} \quad (4)$$

The derivative of a basis function is given by

$$N_{i,p}^k(u) = p \left(\frac{N_{i,p-1}^{(k-1)}(u)}{u_{i+p} - u_i} + \frac{N_{i+1,p-1}^{(k-1)}(u)}{u_{i+p+1} - u_{i+1}} \right) \quad (5)$$

The length of the knot vector is $m+1$ or $n+p+2$ which is determined by the degree p , and the number of control points $n+1$, of the curve.

The B-spline basis functions can be constructed based on the knot vector. Then a system of linear equations can be formed to calculate approximate B-spline curve for the given data points.

$$\begin{aligned} \hat{q}^t &= \begin{bmatrix} \hat{q}_{x0}^t & \hat{q}_{y0}^t \\ \hat{q}_{x1}^t & \hat{q}_{y1}^t \\ \vdots & \vdots \\ \hat{q}_{xM}^t & \hat{q}_{yM}^t \end{bmatrix} \\ &= \begin{bmatrix} N_{0,p}(\bar{u}_0) & N_{1,p}(\bar{u}_0) & \dots & N_{n,p}(\bar{u}_0) \\ N_{0,p}(\bar{u}_1) & N_{1,p}(\bar{u}_1) & \dots & N_{n,p}(\bar{u}_1) \\ \vdots & \vdots & \ddots & \vdots \\ N_{0,p}(\bar{u}_M) & N_{1,p}(\bar{u}_M) & \dots & N_{n,p}(\bar{u}_M) \end{bmatrix} \cdot \begin{bmatrix} P_{x0} & P_{y0} \\ P_{x1} & P_{y1} \\ \vdots & \vdots \\ P_{xn} & P_{yn} \end{bmatrix} \\ \hat{q}_{(M+1)\times 2}^t &= \Phi_{(M+1)\times(n+1)} P_{(n+1)\times 2} \end{aligned} \quad (6)$$

The control points, $P_{(n+1)\times 2}$, are the fit parameters which is calculated by minimising the errors between the given data points and the computed points on the fitted curve by

$$e^t = q^t - \hat{q}^t = q^t - \Phi P \quad (7)$$

The least squares objective function becomes the minimisation problem, which can be solved by setting the derivative of the objective function concerning the minimisation parameter, the control points, $\frac{\partial J_L}{\partial P}$ to zero.

$$J_L = \frac{1}{2}(e^t)^T e^t = \frac{1}{2}(q^t - \Phi P)^T (q^t - \Phi P) \quad (8)$$

$$\begin{cases} \frac{\partial J_L}{\partial P} \\ P \end{cases} = -\Phi^T (q^t - \Phi P) = 0 \quad (9)$$

B. Offset Curve Generation

To improve a product model's geometrical quality, for each layer, the contour and its offset contour curve are combined to generate the path. An example is given in Fig. 3. The offset distance is determined by the diameter of the printer head and the overlapping rate between two neighbour tool-path lines.

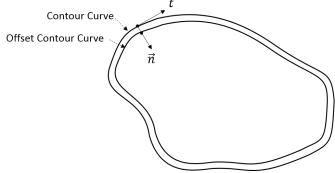


Fig. 3: An example for computing the offset contour curve

1) Offset Point search: The discrete points are sampled adaptive on the given contour curve and ensure that the chord error caused by sampling does not exceed the given limit. The sample length is determined by Equ. 10. ε is the given chord error limit.

$$ds = 2R * \arccos(1 - \varepsilon * r/R); \quad (10)$$

A set of circles are generated by taking the sample points as the centre and offset distance as the radius. Then the common tangent of adjacent circles is identified. As a result, each circle, taking C_i in Fig. 4 as an example, has two tangent points p_{t1} and p_{t2} . Then the offset point p'_i is calculated. The procedure is performed for all the discrete points until all the offset points are obtained. These offset points are used to construct the offset curve.

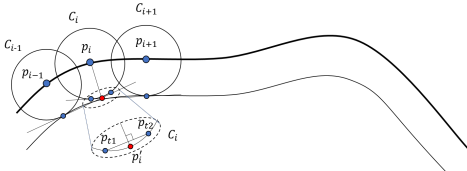


Fig. 4: The algorithm for computing offset contour curve

2) Deal with self-intersection case: However, the self-intersection will occur when the offset distance larger than the radius of curvature of the contour curve as shown in Fig. 5a.

The self-intersecting points are identified by check if an offset point located in an offset circle as shown in Fig. 5b. A k-d tree of the circle centre points is built firstly. Then, for

each offset point, the nearest circle centre point is searched by a k-d tree. If the nearest distance between the offset and its nearest circle centre points is less than the offset value, the offset point is the bad point which should be removed. Finally, the offset curve is obtained by fitting the remaining points.

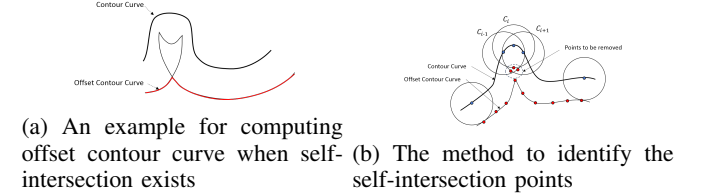


Fig. 5: Self intersection

C. Hybrid process

Process planning refers to the identification of a sequence of operations that will lead to the manufacture of the desired part and generate corresponding control files. This part involves determining the sequences of additive, subtractive processes, defining individual tool paths and process parameters and generating the control files for the system. Compare to the conventional manufacturing process, the advantage of combining the CNC machining and robotic additive manufacturing is that it renders change between additive and subtractive processing possible: the laser realises the powder coating while the milling head realises the machining.

For the given model, the deposition path is generated. Then based on the surface to be machined, the machining path is generated. The operation of the additive and the subtractive process could be either sequentially or alternately which is determined by the geometric features and machining requirements of the workpieces. Finally, an integrated control file is generated based on the sequence of operations, deposition path, machining path as well as process parameters.

V. SYSTEM SETUP

The system involves three subsystems: a robotic AM system, CNC machining system and positioning system. The integration has to be done in such a manner that each subsystem can work independently and the interaction between the systems is done by signal transmission of the upper layer.

To implement the system for achieving these objectives, the hardware designed as shown in Fig. 6. The hardware involving in this system includes a laser deposition system, a 6DoF robot, a positioner system and a 3-axis CNC machine and some other equipment such as cooling equipment, dust removal equipment.

A. Robotic AM system

This station uses laser direct metal deposition(LDMD), which is one of a small proportion of the current range of direct-write methods capable of producing a full density metallic surface layer or volume. The fusion of this idea with that of layered manufacturing led to a technique capable of producing not only surface layers but complex three-dimensional parts

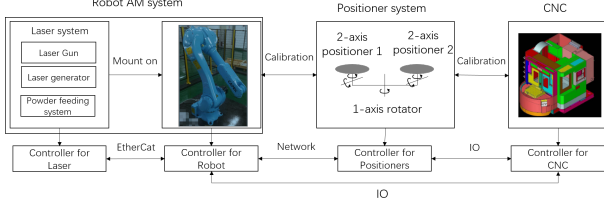


Fig. 6: Hybrid manufacturing system

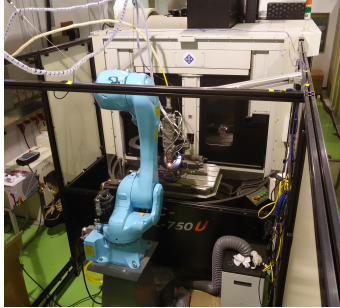


Fig. 7: Hybrid manufacturing system station

with near net shape accuracy. In laser cladding, the laser beam is defocused on the workpiece with selected spot size. The powder coating material is carried by an inert gas through a powder nozzle into the melt pool. The laser optics and powder nozzle are moved across the workpiece surface to deposit single tracks, complete layers or even high-volume build-ups.

In robotic AM system, the hardware includes a CAPEK 6 DoF manipulator[14], laserline LDM series laser system[15] and the GTV powder feeder, type PF[16].

B. Positioning system

The positioner system consists of two 2-axis pointioners and a rotator. These two positioners are mounted on the separate sides of the rotator. At a particular moment, each positioner can cooperate with the manipulator or CNC system to implement its corresponding tasks independently. When it comes to the change of the manufacturing mode, the rotator can swap the location of two positioners.

C. CNC machining system

In this system, a CNC machine APC-MVL-750U[17] is selected to do the material removal process. The CNC machine is allowed to communicate with the robotic AM system and positioning system to complete the cooperative work.

VI. EXPERIMENTS AND CASE STUDY

In this section, to determine the parameters for laser cladding process, several experiments are carried out. Finally, a wheel hub is deposited as a case study to verify both the algorithms and the whole system.

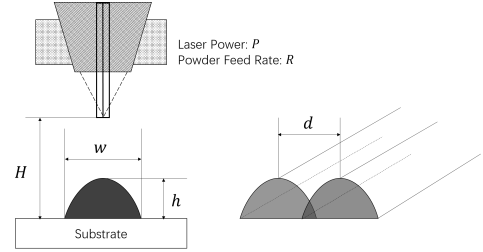


Fig. 8: Laser deposition parameter

A. Experiments

Fig. 8 shows the typical parameters for a laser cladding process with laser height(H), bead height(h), bead width(w), laser power(P) and powder feed rate(R). Laser power(P) and powder feed rate(R) is determined by characteristics of cladding material alloys. The powder used in our experiments is steel powder, and its parameter is shown in Table ???. Then the laser power(P) and powder feed rate(R) are obtained by checking the manual of the laser where $P = 1.28KW$ and $R = 1kg/h$.

The laser height during processing should ensure that the focus of the laser is precisely on the surface of the powder. An experiment is conducted by moving the laser on the plane by continuously increasing its height. The metal material will pile up into line with a varying width which is reduced from large to small and expanded to large again. The appropriate laser height($H = L = 12mm$) is obtained by measuring laser height when printing the thinnest part of the line.

Suitable travel speed of the laser is determined by evaluating the deposition quality of a circle with different travel speed value. A series of experiments are carried out, and the result is shown in Table. I. The experiments show that when the travel speed is equal to $40mm/s$, the deposition generates a good quality circle with the layer height of $0.1mm$.

TABLE I: The deposition result of different travel speed

| No. | Travel speed | Layer Num. | Total Height | Layer Height |
|-----|--------------|------------|--------------|--------------|
| 1 | 20mm/s | 10 | 2.0mm | 0.2mm |
| 2 | 25mm/s | 10 | 1.6mm | 0.16mm |
| 3 | 30mm/s | 10 | 1.3mm | 0.13mm |
| 4 | 40mm/s | 10 | 1.0mm | 0.1mm |
| 5 | 50mm/s | 10 | 0.8mm | 0.08mm |
| 6 | 75mm/s | 10 | 0.5mm | 0.05mm |
| 7 | 100mm/s | 10 | 0.2mm | 0.02mm |
| 8 | 125mm/s | 10 | 0.1mm | 0.01mm |

The bead width is $2.3mm$ by measurement when the travel speed is $40mm/s$. Experiments is carried out by cladding a circle to determine the offset distance d . The experiments show that the offset distance $d = 2mm$ is an ideal parameter.

Finally, the process parameters are determined as shown in Table II, and these parameters are applied in the following deposition experiments.

TABLE II: Laser deposition parameters

| Laser power | Powder feed rate | Laser height | travel speed | Bead height | Bead width |
|-------------|------------------|--------------|--------------|-------------|------------|
| 1.28kw | 1kg/h | 12mm | 200m/s | 0.1mm | 2mm |

B. Case study

A wheel hub is selected as a workpiece to manufacture in the hybrid system. The model is partitioned into four parts based on its geometric features.

Fig. 9 illustrates the process steps. Firstly, the cone base is deposited by robotic AM system, and then the cylinder is cladding on it as well as the disc on its top. Finally, the six cylindrical protrusion is deposited on the surface of the cone. During the deposition, the laser gun should be always vertically downward, so the positioner need to change the attitude of the model exactly. When each part of the workpiece is deposited, the positioner system will send it into CNC machine for machining process and then rotate it back for subsequent deposition.

Fig. 9 gives the intermediate product of and the finally outcome of the wheel model.

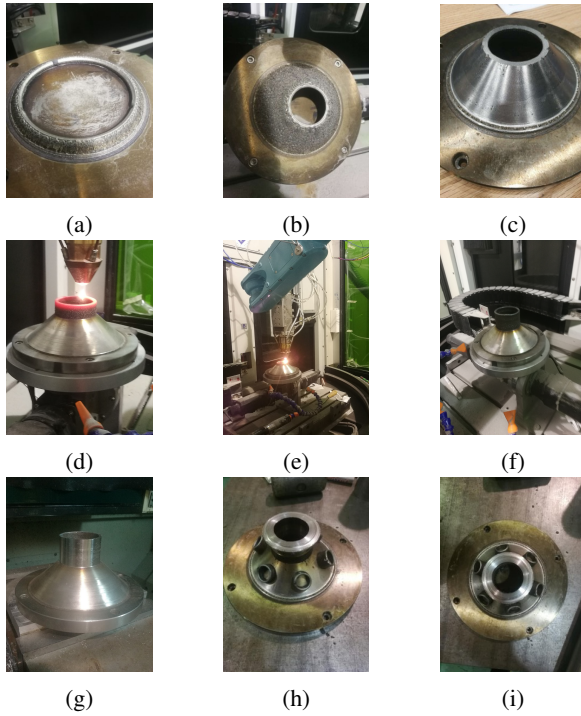


Fig. 9: The manufacturing result of the wheel model

VII. CONCLUSIONS

The main contribution of this article is to propose a hybrid manufacturing process which combines the best features of both robotic additive manufacturing and CNC machining approaches. The method involves the tool path generation algorithm and the actual workstation construction. The critical steps of the tool path generation algorithm are mesh slicing and curve offset algorithm. The workstation consists of several subsystems to work together to achieve processing tasks. For a

given workpiece, this method provides a hybrid manufacturing process to assign adding and subtracting material tasks to the robotic additive manufacturing system and the CNC machine, and other subsystems assist in the completion of the works. Finally, an industrial case carried out by depositing a wheel prove the viability of the hybrid system.

REFERENCES

- [1] J. N. Pires and A. S. Azar, "Advances in robotics for additive/hybrid manufacturing: robot control, speech interface and path planning," *Industrial Robot: An International Journal*, 2018.
- [2] G. Q. Zhang, W. Mondesir, C. Martinez, X. Li, T. A. Fuhlbrigge, and H. Bheda, "Robotic additive manufacturing along curved surfaces-a step towards free-form fabrication," in *Robotics and Biomimetics (ROBIO), 2015 IEEE International Conference on*, pp. 721–726, IEEE, 2015.
- [3] D. Ding, Z. Pan, D. Cuiuri, and H. Li, "A multi-bead overlapping model for robotic wire and arc additive manufacturing (waam)," *Robotics and Computer-Integrated Manufacturing*, vol. 31, pp. 101–110, 2015.
- [4] G. Q. Zhang, X. Li, R. Boca, J. Newkirk, B. Zhang, T. A. Fuhlbrigge, H. K. Feng, and N. J. Hunt, "Use of industrial robots in additive manufacturing-a survey and feasibility study," in *ISR/Robotik 2014; 41st International Symposium on Robotics; Proceedings of*, pp. 1–6, VDE, 2014.
- [5] S. Suryakumar, K. Karunakaran, A. Bernard, U. Chandrasekhar, N. Raghavender, and D. Sharma, "Weld bead modeling and process optimization in hybrid layered manufacturing," *Computer-Aided Design*, vol. 43, no. 4, pp. 331–344, 2011.
- [6] K. Karunakaran, S. Suryakumar, V. Pushpa, and S. Akula, "Low cost integration of additive and subtractive processes for hybrid layered manufacturing," *Robotics and Computer-Integrated Manufacturing*, vol. 26, no. 5, pp. 490–499, 2010.
- [7] A. Shamir, "A survey on mesh segmentation techniques," in *Computer graphics forum*, vol. 27, pp. 1539–1556, Wiley Online Library, 2008.
- [8] L. Shapira, A. Shamir, and D. Cohen-Or, "Consistent mesh partitioning and skeletonisation using the shape diameter function," *The Visual Computer*, vol. 24, no. 4, p. 249, 2008.
- [9] K. Chalasani, B. Grogan, A. Bagchi, C. Jara-Almonte, A. Ogale, and R. Dooley, "An algorithm to slice 3d shapes for reconstruction in prototyping systems," in *Proceedings of the 1991 ASME Computers in Engineering Conference*, pp. 209–216, 1991.
- [10] I. Wald and V. Havran, "On building fast kd-trees for ray tracing, and on doing that in $O(n \log n)$," in *Interactive Ray Tracing 2006, IEEE Symposium on*, pp. 61–69, IEEE, 2006.
- [11] L. Piegl and W. Tiller, *The NURBS book*. Springer Science & Business Media, 2012.
- [12] A. Gasser, G. Backes, I. Kelbassa, A. Weisheit, and K. Wissenbach, "Laser additive manufacturing: Laser metal deposition (lmd) and selective laser melting (slm) in turbo-engine applications," *Laser Technik Journal*, vol. 7, no. 2, pp. 58–63, 2010.
- [13] W. King, A. Anderson, R. Ferencz, N. Hodge, C. Kamath, S. Khairallah, and A. Rubenchik, "Laser powder bed fusion additive manufacturing of metals: physics, computational, and materials challenges," *Applied Physics Reviews*, vol. 2, no. 4, p. 041304, 2015.
- [14] "Capek ca20n product detail." http://www.capekrobotics.com/gjqr/info_21.aspx?itemid=273. Accessed: 2018-08-06.
- [15] "Laserline ldm series product detail." <https://www.laserline.com/lmseries/>. Accessed: 2018-08-06.
- [16] "The gtv powder feeder, type pf product detail." <https://www.gtv-mbh.com/equipment-systems/powder-feeder/>. Accessed: 2018-08-06.
- [17] "Cnc machine apc-mvl-750u product detail." <http://www.marmaracnc.com/urun-detay.php?id=24>. Accessed: 2018-08-06.